

IC/95/225
INTERNAL REPORT
(Limited Distribution)

International Atomic Energy Agency
and
United Nations Educational Scientific and Cultural Organization
INTERNATIONAL CENTRE FOR THEORETICAL PHYSICS

**NUMERICAL MODELING OF BLOCK STRUCTURE DYNAMICS:
APPLICATION TO THE VRANCEA REGION
AND STUDY OF EARTHQUAKE SEQUENCES
IN THE SYNTHETIC CATALOGS**

A.A. Soloviev and I.A. Vorobieva
International Centre for Theoretical Physics, Trieste, Italy
and
International Institute of Earthquake Prediction Theory
and Mathematical Geophysics, Russian Academy of Sciences,
Moscow, Russian Federation.

MIRAMARE - TRIESTE
August 1995

ABSTRACT

A seismically active region is represented as a system of absolutely rigid blocks divided by infinitely thin plane faults. The interaction of the blocks along the fault planes and with the underlying medium is viscous-elastic. The system of blocks moves as a consequence of prescribed motion of boundary blocks and the underlying medium. When for some part of a fault plane the stress surpasses a certain strength level a stress-drop ("a failure") occurs. It can cause a failure for other parts of fault planes. The failures are considered as earthquakes. As a result of the numerical simulation a synthetic earthquake catalog is produced.

This procedure is applied for numerical modeling of dynamics of the block structure approximating the tectonic structure of the Vrancea region. By numerical experiments the values of the model parameters were obtained which supplied the synthetic earthquake catalog with the space distribution of epicenters close to the real distribution of the earthquake epicenters in the Vrancea region. The frequency-magnitude relations (Gutenberg-Richter curves) obtained for the synthetic and real catalogs have some common features.

The sequences of earthquakes arising in the model are studied for some artificial structures. It is found that "foreshocks", "main shocks", and "aftershocks" could be detected among earthquakes forming the sequences. The features of aftershocks, foreshocks, and catalogs of main shocks are analysed.

DESCRIPTION OF THE MODEL

A seismically active region is represented as a system of absolutely rigid blocks divided by infinitely thin plane faults.

Blocks interact between themselves and with the underlying medium. The system of blocks moves as a consequence of prescribed motion of boundary blocks and the underlying medium. All deformation takes place in the fault zones and the block bottoms separating the blocks and the underlying medium. The relative displacements of the blocks take place along the fault planes and are supposed to be infinitely small compared with geometric size of the structure. The blocks are in viscous-elastic interaction with the underlying medium. The dependence of stress on the value of relative displacement is assumed to be linear elastic.

The motion of the blocks of the structure is determined in such a way that the system is in quasistatic equilibrium state.

The interaction of the blocks along the fault planes is viscous-elastic ("normal state") while the stress is below a certain strength level. When the level is surpassed for some part of a fault plane a stress-drop ("a failure") occurs. It can cause a failure for other parts of fault planes. Each sequence of such failures is considered as an earthquake. After the earthquake the corresponding parts of the fault planes are in creep state which lasts until the stress falls below a certain other level. In this state the interaction along the fault plane is viscous-elastic but the values of constants are different from those in normal state. As a result of the numerical simulation a synthetic earthquake catalog is produced.

Block structure geometry. A layer with thickness H between two horizontal planes is considered. A block structure is a limited and connected part of this layer. A lateral boundary of the block structure consists of parts of planes intersecting the layer. Division of the structure into blocks is also accomplished by planes intersecting the layer. Parts of these planes which are inside the block structure and lateral facets of it are called "faults".

Block structure geometry is defined by lines of intersection between the faults and the upper plane (they will also be called faults below) and by angles of dip for the fault planes. It is considered that three or more faults cannot have a common point on

the upper plane. A common point of two faults is called "a vertex". A line of intersection of the fault planes ("a rib") determines crossing the lower plane the position of the vertex on it. A part of a fault between two ribs corresponding to successive vertices on the fault is called "a segment". The segment shape is a trapezium. Common parts of the block with the upper and lower planes are polygons. The common part of the block with the lower plane is called "a bottom".

It is considered that "boundary blocks" adjoin to the structure. A continuous part of the structure boundary between two ribs corresponds to the boundary block.

Block movement. The blocks are assumed to be rigid and all their relative displacements take place along the bounding fault planes. Interaction of the blocks with the underlying medium takes place along the lower plane.

The movements of the boundaries of the block structure (the boundary blocks) and the medium underlying the blocks is assumed to be an external force on the structure. The rates of these movements are considered to be horizontal and known.

The non-dimensional time is used in the model. Therefore all quantities dimensions of which have to include the time are considered to be referred to one unit of the non-dimensional time and their dimensions do not contain the unit of time measurement. For example in the model velocities are measured in the units of the length and the velocity of 5 cm means 5 cm for one unit of the non-dimensional time. When interpreting results a selected real value is given to one unit of the non-dimensional time. For example if one unit of the non-dimensional time is considered to be one year then the velocity of 5 cm specified for the model means 5 cm/year.

At every moment of time the displacements of the blocks are defined so that the structure is in a quasistatic equilibrium.

All displacements are supposed to be infinitely small compared with block size.

Interaction between the blocks and the underlying medium. The elastic force which is due to relative displacement of the block and the underlying medium at some point of the block bottom is supposed to be proportional to the difference between the total relative displacement vector and the vector of slippage (inelastic displacement) at the point.

The specific elastic force $f^u = (f_x^u, f_y^u)$ acting at the point with coordinates (X, Y) at some moment t is defined by

$$\begin{aligned} f_x^u &= K_u(x - x_u - (Y - Y_c)(\varphi - \varphi_u) - x_a), \\ f_y^u &= K_u(y - y_u + (X - X_c)(\varphi - \varphi_u) - y_a). \end{aligned} \quad (1)$$

Here X_c, Y_c are the coordinates of the geometrical center of the block bottom; (x_u, y_u) and φ_u are the shear vector and the angle of rotation around the geometrical center of the block bottom for the underlying medium at the moment t ; (x, y) and φ are the shear vector of the block and the angle of its rotation around the geometrical center of its bottom at time t ; (x_a, y_a) is the inelastic displacement vector at the point at time t .

The evolution of the inelastic displacement at the point is described by the equations

$$\frac{dx_a}{dt} = V_u f_x^u, \quad \frac{dy_a}{dt} = V_u f_y^u. \quad (2)$$

The coefficients K_u and V_u in (1) and (2) may be different for different blocks.

Interaction between blocks along fault planes. At time t at some point of the fault plane separating blocks numbered i and j (the block numbered i is on the left and that numbered j is on the right of the fault) the components $\Delta x, \Delta y$ of the relative displacement of the blocks are defined by

$$\begin{aligned} \Delta x &= x_i - x_j - (Y - Y_c^i)\varphi_i + (Y - Y_c^j)\varphi_j, \\ \Delta y &= y_i - y_j + (X - X_c^i)\varphi_i - (X - X_c^j)\varphi_j. \end{aligned} \quad (3)$$

Here $X_c^i, Y_c^i, X_c^j, Y_c^j$ are the coordinates of the geometrical centers of the block bottoms; $(x_i, y_i), (x_j, y_j)$ are the shear vectors of the blocks at time t ; φ_i, φ_j are the angles of block rotation around the geometrical centers of their bottoms at time t .

In accordance with the assumption that relative block displacements take place only along fault planes, the displacements along the fault plane are connected with the horizontal relative displacement by

$$\begin{aligned} \Delta_t &= e_x \Delta x + e_y \Delta y, \\ \Delta_l &= \frac{\Delta_n}{\cos \alpha}, \quad \text{where } \Delta_n = e_x \Delta y - e_y \Delta x. \end{aligned} \quad (4)$$

Here Δ_t, Δ_l are the displacements along the fault plane parallel (Δ_t) and normal (Δ_l) to the fault line on the upper plane; (e_x, e_y) is the unit vector along the fault line on the upper plane; α is the angle of dip for the fault plane; Δ_n is the horizontal displacement normal to the fault line on the upper plane.

The density of the elastic force $f = (f_t, f_l)$ acting along the fault plane at the point is defined by

$$\begin{aligned} f_t &= K(\Delta_t - \delta_t), \\ f_l &= K(\Delta_l - \delta_l). \end{aligned} \quad (5)$$

Here δ_t, δ_l are inelastic displacements along the fault plane at the point at time t parallel (δ_t) and normal (δ_l) to the fault line on the upper plane.

The evolution of the inelastic displacement at the point is described by the equations

$$\frac{d\delta_t}{dt} = V f_t, \quad \frac{d\delta_l}{dt} = V f_l. \quad (6)$$

The coefficients K and V in (5) and (6) may be different for different faults.

In addition to the elastic force, there is also a reaction force which is normal to the fault plane. But this force does no work, because all relative movements are tangent to the fault plane. The density of elastic energy at the point is equal to

$$e = (f_t(\Delta_t - \delta_t) + f_l(\Delta_l - \delta_l))/2. \quad (7)$$

From (4) and (7) the elastic force density horizontal component normal to the fault line on the upper plane can be obtained. The component is equal to

$$f_n = \frac{\partial e}{\partial \Delta_n} = \frac{f_l}{\cos \alpha}. \quad (8)$$

Formula (8) confirms that the reaction force is normal to the

fault plane. The density of the reaction force is equal to

$$P_0 = f_i \operatorname{tg} \alpha. \quad (9)$$

The formulas given above are also valid for the boundary faults. In this case one of the blocks separated by the fault is the boundary block. The movement of these blocks is described by their shears and rotations around the coordinate origin. Therefore the coordinates of the geometrical center of the block bottom in (3) are zero for the boundary block. For example, if a block numbered j is the boundary block, then $X_c^j = Y_c^j = 0$ in (3).

Equilibrium equations. The components of the shear vectors of the blocks and the angles of their rotation around the geometrical centers of the bottoms are found from the condition that the total force and the total moment of forces acting on each block are equal to zero. This is the condition of the quasi-static equilibrium of the system and at the same time the condition of minimum energy.

In accordance with formulas given above the system of equations which describes the equilibrium has the following form

$$Az = b, \quad (10)$$

where the components of the unknown vector $z = (z_1, z_2, \dots, z_{3n})$ are the components of the shear vectors of the blocks and the angles of their rotation around the geometrical centers of the bottoms (n is the number of blocks), i.e. $z_{3m-1} = x_m$, $z_{3m-2} = y_m$, $z_{3m-3} = \varphi_m$ (m is the number of the block, $m = 0, 1, \dots, n-1$).

For each block the moment of forces is calculated relative to the geometrical center of its bottom.

Discretization. Time discretization is performed by introducing a time step Δt . The block structure state is considered for discrete moments of time $t_i = t_0 + i\Delta t$ ($i = 1, 2, \dots$), where t_0 is the initial moment. Transition from the state at t_i to the state at t_{i+1} is made as follows. First, new values of the inelastic displacements $x_a, y_a, \delta_a, \delta_l$ are calculated from equations (2) and (6). Next the shear vectors and the rotation angles at t_{i+1} for the boundary blocks and the underlying medium are calculated. Then the components of b in equations (10) are calculated and the equations are used to define the shear vectors and the angles of rotation for the blocks. As the elements of A in (10) do not depend on time, the matrix A and the associated inverse matrix can be calculated just once at the beginning of the calculation.

Space discretization is defined by the parameter ϵ . Discretization is made for the surfaces of fault segments and block bottoms. Discretization of a fault segment is performed as follows. As noted above any fault segment is a trapezium. Let a and b be the bases of the trapezium. The trapezium height h is given by $h = H/\sin \alpha$, where H is the thickness of the layer, α is the dip angle of the fault plane. Let

$$n_1 = \text{ENTIRE}(h/\epsilon) + 1, \quad n_2 = \text{ENTIRE}(\max(a,b)/\epsilon) + 1.$$

The trapezium is divided into $n_1 n_2$ small trapeziums by two groups of lines inside it: $n_1 - 1$ lines parallel to the trapezium bases spaced at intervals of h/n_1 , and $n_2 - 1$ lines connecting the points spaced at intervals of a/n_2 and b/n_2 , respectively, on the bases. The small trapeziums obtained will be called cells. The coordinates X, Y of the center of the mean line of the cell are assigned to all its points. The inelastic displacements δ_a, δ_l are supposed to be the same for all points of the cell.

A block bottom is a polygon. Before discretization it is divided into trapeziums (triangles) by lines passing through its vertices and parallel to the Y axis. The discretization of these trapeziums (triangles) is performed in the same way as in the case of fault segments. The small trapeziums (triangles) are also called cells. For all points of the cell the coordinates X, Y and the inelastic displacements x_a, y_a are supposed to be the same.

Earthquake and creep. Denote

$$\kappa = \frac{\|(f_e, f_l)\|}{P - P_0} \quad (11)$$

where (f_e, f_l) is the density vector of the elastic force given by (5), P is the difference between lithostatic and hydrostatic pressure which has the same value for all faults, P_0 is the density of the reaction force which is given by (9).

For each fault the values of the following three levels are indicated

$$B > H_f \geq H_s.$$

The initial conditions for numerical simulation of block structure dynamics are supposed to satisfy the inequality $\kappa < B$ for all cells of the fault segments. If at some moment t_i the value of κ in any cell of a fault segment reaches the level B , failure ("earthquake") occurs. Failure means slippage during which the inelastic displacements δ_a, δ_l in the cell change abruptly to reduce

the value of κ to the level H_t .

The new values of the inelastic displacements in the cell are calculated from

$$\delta_t^* = \delta_t + \gamma f_t, \quad \delta_l^* = \delta_l + \gamma f_l \quad (12)$$

where δ_t , δ_l , f_t , f_l are the inelastic displacements and the components of the elastic force density vector just before the failure. The coefficient γ is given by

$$\gamma = \left[1 - \frac{PH_t}{\sqrt{f_t^2 + f_l^2 + H_t f_l \operatorname{tg} \alpha}} \right] \frac{1}{K} \quad (13)$$

It follows from formulas (5), (9), (11)-(13) that after calculation of the new values of the inelastic displacements the value of κ in the cell equals the level H_t .

After calculating the new values of inelastic displacements for the all failed cells, the new components of the vector b are calculated and from the system of equations (10) the shear vectors and the angles of rotation for the blocks are found. If for some cell of the fault segments $\kappa \geq B$, the procedure given above is repeated for this cell (or cells). Otherwise the state of the block structure at time t_{i+1} is calculated in the ordinary manner. Note that different times could be attributed to the failures occurring on different steps of the procedure given above: if the procedure consists of p steps the time $t_i + (j - 1)\delta t$ could be attributed to the failures occurring on the j th step. The value of δt is selected to satisfy the condition $p\delta t < \Delta t$.

The cells in which failures occurred at the same time are united to form an earthquake. Selection of the cells to be united can be made by different ways: the all cells of the structure in which failures occurred at this time, only those of them which belong to a connected set of segments or to a connected set of segments of the same fault or to the same segment etc. The parameters of the earthquake are defined as follows: time is $t_i + (j - 1)\delta t$; coordinates and depth are weighted sums of coordinates and depths of the cells included in the earthquake (the weights of the cells are their squares divided by the sum of squares of these cells); magnitude is calculated as

$$M = D \lg S + E, \quad (14)$$

where D and E are constants; S is the sum of the squares of the

cells (in km^2) included in the earthquake.

The cells in which failures occurred are considered to be in the creep state. It means that for these cells the parameter V_* ($V_* \geq V$) is used instead of V in equations (6) which describe the evolution of inelastic displacement. The values of V_* may be different for different faults. A cell is in the creep state while $\kappa > H_*$ for it. When $\kappa \leq H_*$, the cell returns to the ordinary state and henceforth the parameter V is used in (6) for this cell.

NUMERICAL MODELING OF BLOCK STRUCTURE DYNAMICS FOR VRANCEA REGION

In accordance with [1] the main structure elements of the Vrancea region are: East-European plate; Moesian, Black Sea, and Intra-Alpine (Pannonian-Carpathian) subplates. These elements are shown in Figures 1 and 2 which are taken from [2].

The fault which separates the East-European plate from the Intra-Alpine and Black Sea subplates has the dip angle which is less essentially than 90° being measured on the hand of the subplates. The fault which separates the Intra-Alpine and Black Sea subplates also has the dip angle which is less essentially than 90° being measured on the hand of the Intra-Alpine subplate.

The main directions of plate movement are shown in Figures 1 and 2.

This information is enough to specify a block structure which could be considered as a rough approximation of the Vrancea region and movements which can be used for numerical simulation of dynamics of this block structure.

Block structures used for numerical simulation. In order to approximate the structure of the Vrancea region the block structure was specified. The configuration of its faults on the upper plane is presented in Figure 3.

For the structure the point with the geographic coordinates 44.2°N and 26.1°E was selected as the coordinate origin. The X axis is the east-looking parallel passing through the coordinate origin. The Y axis is the north-looking meridian passing through the coordinate origin.

The thickness of the layer is $H = 200$ km, which corresponds the more deep earthquakes in the Vrancea region.

The vertices of the block structure with the numbers 1-7 have the following coordinates (in 10km): (-33; -21), (-27; 48), (45; 9), (11; -27), (0; 27), (0; 9), (-21; 7.5).

The vertices 8-11 have the following relative positions on the faults to which they belong: 0.3, 0.33, 0.5, 0.667. The relative position of the vertex is the ratio of the distance from the initial point of the fault to the vertex to the length of the fault. The vertices 1, 5, 3, and 10 are considered to be initial for the faults while the relative positions of the vertices 8-11 are determined.

TABLE 1 Faults

#	Vertices	Dip angle	K , bars/cm	V , cm/bars	V_s , cm/bars	B	H_f	H_s
1	1, 8, 2	45°	0	0	0	0.1	0.085	0.07
2	2, 5	120°	1	0.5	1	0.1	0.085	0.07
3	5, 9, 3	120°	1	0.05	0.1	0.1	0.085	0.07
4	3, 10, 4	45°	0	0	0	0.1	0.085	0.07
5	4, 1	45°	0	0	0	0.1	0.085	0.07
6	10, 11, 6	100°	1	0.05	0.1	0.1	0.085	0.07
7	6, 7	100°	1	0.05	0.1	0.1	0.085	0.07
8	7, 8,	100°	1	0.05	0.1	0.1	0.085	0.07
9	11, 9	70°	1	0.02	0.04	0.1	0.085	0.07

The structure has 9 faults. The values of the constants for these faults are given in Table 1. The values of constants for 3 blocks forming the structure are given in Table 2.

The movement of the underlying medium is specified to be progressive. The components of the velocity (V_x , V_y) of this movement are specified for blocks in accordance with the directions of the main movements of the Vrancea region shown in Figures 1 and 2 and are also given in Table 2. Note that the non-dimensional time is used in numerical simulation and the values of V and V_s in Table 1 as well as values of V_u and velocities below correspond to the non-dimensional time.

It is specified that the boundary which consists of the faults 2 and 3 moves progressively with the same velocity:

$$V_x = -16 \text{ cm}, \quad V_y = -5 \text{ cm}.$$

The boundary faults 1, 4, and 5 does not move. Note that $K = 0$ for these faults (Table 1) and therefore in accordance with formulas (5) and (8) all forces in these faults are equal to zero.

The difference between lithostatic and hydrostatic pressure P in formula (11) equals 2 Kbars.

Earthquake magnitude is calculated with the following values of

TABLE 2 Blocks

#	Vertices	K_u , bars/cm	V_u , cm/bars	V_x , cm	V_y , cm
1	2, 8, 7, 6, 11, 9, 5	1	0.05	25	0
2	3, 9, 11, 10	1	0.05	-15	7
3	4, 10, 11, 6, 7, 8, 1	1	0.05	-20	5

the constants in (14):

$$D = 0.98; \quad E = 3.93. \quad (15)$$

The values of the parameters of discretization are the following:

$$\Delta t = 0.001, \quad c = 7.5 \text{ km.}$$

Seismicity of Vrancea. The Vrancea seismoactive region is characterized by relatively small size, intermediate deep earthquakes and high level of seismic activity. In our century 4 catastrophic earthquakes with magnitude 7 or more had occurred (Table 3).

There are several earthquakes catalogs for Vrancea region. The catalog [3] of Romanian local network covers the period of time from 1900/01/01 till 1979/12/31. The catalog [4] "Earthquakes in the USSR" covers period from 1962/01/01 till 1990/12/31. The catalog [5] of Romanian local network covers the period from 1980/01/01 till 1995/04/01; for the period of time before 1994 it contains only intermediate deep earthquakes (depth more than 60 km); in order to complete it by the shallow seismicity the data from the worldwide NEIC catalog were used.

The compiled catalog is used below. It consists of the three parts: [3] for the period 1900-1961, [4] for the period 1962-1979, and [5] completed by the shallow seismicity data from NEIC for the period 1980-1995.

Comparison of synthetic and real catalogs. The synthetic earthquake catalog was obtained for the structure with zero initial conditions for the period of 200 units of non-dimensional time.

The catalog contains 9439 events with magnitudes between 5.05 and 7.6. The minimal value of magnitude corresponds to the minimum square of one cell in accordance with (14) and (15). The maximal value of magnitude in the synthetic catalog is close to one ($M = 7.4$) in the real catalog.

TABLE 3 Strong earthquakes of Vrancea, 1900 - 1995

Date	Time	Hypocenter			Magnitude
		latitude	longitude	depth (km)	
1940/11/10	1.39	45.80°N	26.70°E	133	7.4
1977/03/04	19.21	45.78°N	26.80°E	110	7.2
1986/08/30	21.28	45.51°N	26.47°E	150	7.0
1990/05/30	10.40	45.83°N	26.74°E	110	7.0

The map with the distribution of epicenters in the synthetic catalog is given in Figure 4. The real seismicity is presented in Figure 5.

The main part of events occurred on the fault 9 (the cluster A in Figure 4), which corresponds to the subduction zone of Vrancea, where main real seismicity is concentrated (the cluster A in Figure 5). All strong earthquakes of the synthetic catalog with $M \geq 6.7$ are concentrated here, and the same phenomenon is seen in the distribution of the real seismicity.

The part of the intermediate strong events had occurred on the fault 6 of the block structure. It looks like a cluster of epicenters situated to the south-west from the main seismicity and separated from it by a non-seismic zone (the cluster B in Figure 4). The analogous cluster of epicenters we can see on the map of real seismicity (the cluster B in Figure 5).

The third cluster of events (the cluster C in Figure 4) is situated on the fault 8 of the block structure and it corresponds to the cluster C of the real seismicity in Figure 5.

On the map of the real seismicity (Fig.5) there are several more clusters of epicenters which are absent in the synthetic catalog. It caused by the reason that only few main seismic faults of Vrancea region were used. The simulation of the more likelihood distribution of epicenters needs more detail description of the real faults system by the block structure. However the considered very simple structure consisting of 3 blocks only, reflects main features of the spatial distribution of the real seismicity.

Temporal characteristics of the synthetic catalog are shown by the distribution of the number of earthquakes by magnitude and time given in Table 4. Simulating was started from zero initial condition and some period of time is needed for the quasi-stabilization of the stresses. It is possible to estimate the time of stabilization using the histogram time-magnitude. Starting from 60 units of the non-dimensional time the distribution of the number of events by the magnitude and the time looks stable. The stable part of the synthetic catalog from 60 to 200 units of the non-dimensional time is only considered below.

The Gutenberg-Richter law on the frequency-of-occurrence for the real seismicity is that logarithm of the number of earthquakes depends linearly on the magnitude. The frequency-of-occurrence

TABLE 4 Histogram of the dependence of the number of events in the synthetic catalog on the non-dimensional time for different magnitude intervals

Time units	Magnitude										Total	
	5.00	5.40	5.80	6.20	6.60	7.00	7.40					
0												0
10		4	15									24
20		101	556	148								846
30	28	102	378	130	60	23	4					725
40	39	66	247	113	83	47	27	7	1			630
50	6	42	205	76	62	36	24	14	5	1		471
60	7	51	227	98	67	26	24	11	7	1	2	522
70	5	42	207	80	58	40	23	8	5	2	3	476
80	8	37	198	87	78	37	20	10	5	1	1	482
90	2	41	201	77	70	43	26	9	2	3	3	478
100	8	42	181	86	68	35	20	11	6	3	1	461
110	9	35	227	81	66	34	17	9	6	2	3	489
120	10	37	210	88	56	29	19	9	4	2	1	465
130	6	39	204	65	69	33	24	5	4	3	2	456
140	7	34	206	80	60	37	15	4	6	2	1	453
150	7	49	221	76	67	32	20	7	6	3	1	492
160	15	37	227	92	64	23	21	9	5	5	1	500
170	12	55	219	62	66	25	19	14	7	1	2	476
180	11	42	192	88	68	23	21	7	9	1	1	463
190	7	55	220	98	81	31	21	7	7	3		530
Total	187	911	4341	1630	1180	558	345	141	77	33	19	15
	9439 events											

graphs for the real Vrancea seismicity and for the synthetic catalog are presented in Figure 6. The graph for the synthetic catalog (the dashed line) looks like linear, moreover, it has approximately the same slope as the graph for the real seismicity (the solid line). One can see that there is a gap in the magnitude interval $6.5 < M < 7.0$ for the real seismicity which is not observed in the synthetic catalog. But this gap in the real seismicity may be caused by a low number of events for a "short" period of time.

By using the frequency-of-occurrence graph and the duration of the real catalog (95 years) the correspondence of the non-dimensional with the real one can be estimated. The result is that 140 units of the non-dimensional time are equivalent approximately to 7000 years or 1 unit may be interpreted as 50 years. It gives the value of the tectonic movement velocities about 5 mm per year.

In accordance with the estimation given above the duration of the synthetic catalog is in 70 times more than of the real catalog. The synthetic catalog was divided into 70 parts and these parts were compared each to other and to the real catalog. The data for 70 parts of the synthetic catalog are presented in Table 5.

The real catalog contains 71 event with $M \geq 5.4$, maximal magnitude is 7.4, and there are 4 strong events (Table 3). The parts of the synthetic catalog contain from 53 to 94 events with $M \geq 5.4$, the average number of events is 68 (Table 5). If the events with $M \geq 6.8$ are considered as strong, then the number of strong earthquakes varies from 0 to 4. There are no strong events in 29 parts, there is one strong event in 20 parts, 2 - in 16 parts, 3 - in 4 parts, and 4 - in 1 part. The maximal magnitude varies from 6.0 to 7.6.

4 strong events (as in the real contemporary seismicity) occur only in the one part of the synthetic catalog. It may mean, that now we live in "active period".

It is interesting to consider the frequency-of-occurrence graphs for the periods without strong earthquakes and for the periods with several strong earthquakes. The graphs for the real catalog (the solid line) and for the synthetic catalog (the dashed line) for the period without strong earthquakes are presented in Figure 7. One can see similar slopes and intensities of the graphs. The graphs for the period with strong earthquakes are presented in Figure 8. There is a gap in the number of earthquakes separating

strong earthquakes, like in the real frequency-of-occurrence graph. Such gap is a typical phenomenon for the periods with several strong shocks (Table 5).

The distribution of the strong ($M \geq 6.8$) earthquakes in the synthetic catalog for the all period of time (140 units or 7000 years) presented in Figure 9 shows that the behavior of the strong seismicity is different for the different periods of time.

For the period 70 - 120 units the periodical occurrence of the groups of strong earthquakes with the period about 6-7 units can be observed, which corresponds 300 - 350 years of the real time. Note, that the unique period of the synthetic catalog with 4 strong shocks belongs to this period.

For the next period of 120 - 140 units the periodic occurrence of a single strong earthquake with the period about 2 units or 100 years is typical. For the rest periods of time there are not any periodicity in the occurrence of the strong earthquakes.

These data show that it is necessary to be careful while using seismic cycle for prediction of a future occurrence of a strong earthquake because the available observations cover only the short period of time.

Conclusion. The results listed above show that there is possibility to obtain a synthetic catalog having the similar features with the real earthquake catalog of the Vrancea region. The values of the parameters of the model for which the correspondence between the synthetic and real catalogs is achieved could be useful for estimation of the velocities of the tectonic movements and the values of the physical parameters connected with the processes in the fault zones. If the relevant segment of the synthetic catalog which approximate the real seismic flow with the sufficient accuracy is found then the part of the synthetic catalog just after this segment could be used to estimate the future behavior of the seismicity of the region.

TABLE 5 Data for 70 parts of the synthetic catalog

#	Magnitude										Total Strong M>=6.8	Strong Mmax			
	5.4	5.6	5.8	6.0	6.2	6.4	6.6	6.8	7.0	7.2			7.4	7.6	
1	22	18	17	5	5	4							71	0	6.4
2	25	18	9	2	2	2				1			59	1	7.2
3	26	30	18	9	6	3	1			1			94	1	7.1
4	25	12	8	8	5	4							62	0	6.6
5	31	20	15	2	6	2	2	1	1				80	2	7.0
6	24	14	5	10	2	2	3	1					61	1	6.8
7	19	20	12	12	6	2			1				72	1	7.0
8	22	8	13	2	8	2	1		1				57	1	7.0
9	25	19	10	8	6		3						71	0	6.6
10	23	19	18	8	1	2	1	1	1				74	2	7.1
11	33	15	14	9	3	1							87	0	6.4
12	21	25	16	2	3	3	1						71	0	6.6
13	22	19	11	10	4		1		1	1			69	2	7.2
14	22	13	24	9	6	1	1						76	0	6.6
15	20	15	13	7	4	3	2						64	0	6.6
16	22	15	18	5	9	2		1	2	1			75	4	7.2
17	25	12	15	6	2	2	1						63	0	6.6
18	23	18	9	10	7	1	1						69	0	6.6
19	20	19	12	10	5	2		2	1				71	3	7.1
20	23	13	16	12	3	2							69	0	6.4
21	21	12	12	10	1	2	1						59	0	6.6
22	20	24	13	7	5		1	2					72	2	6.9
23	18	12	9	3	4	1	4	1	1				53	2	7.0
24	22	21	14	7	6	4							74	0	6.4
25	21	17	20	8	4	4							74	0	6.4
26	30	19	14	8	2	3	2						78	0	6.6
27	30	10	17	5	4	2	2			2			72	2	7.3
28	16	15	10	9	4	2		1		1			58	2	7.2
29	23	17	14	6	5	1	1	1					68	1	6.8
30	30	30	11	6	2	1	1						71	0	6.6
31	21	19	7	6	2	2		1	1				59	2	7.0
32	17	19	8	5	4	2		1			1		57	2	7.4
33	19	14	11	4	3	1			1				53	1	7.0
34	24	15	17	6	7	1		1					71	1	6.9
35	20	21	13	8	3	3		1					69	1	6.8
36	23	17	19	6	3	2	2						72	0	6.6
37	28	17	4	7	7	1	1		1	2			68	3	7.3
38	31	7	18	4	7	1		1					69	1	6.8
39	17	11	12	8	3	1	1	1					54	1	6.9
40	26	13	16	8	4			1	1				69	2	7.1
41	22	13	12	11	1	1		1	1				62	2	7.0
42	18	18	10	8	3	1	1			1			60	1	7.3
43	24	15	13	6	2	1	2	1					64	1	6.8
44	31	20	11	8	4		2						76	0	6.6
45	22	14	14	4	5	1	1						61	0	6.6
46	25	17	14	8	1	1	3	1		1			71	2	7.2
47	24	16	17	6	4	2	2		1				71	1	7.0
48	25	14	12	6	4	1			2		1		65	3	7.2
49	26	19	11	9	2	2							69	0	6.4
50	26	10	13	3	9	1	1			1			54	1	7.2
51	20	18	19	6	3	3							69	0	6.4
52	31	20	5	3	2	1	3	1		1			67	2	7.2
53	28	14	9	7	3	1							62	0	6.4
54	27	18	15	4	6	2		2	1				75	3	7.0
55	30	22	16	3	7	2	2	2					84	2	6.9
56	27	5	11	2	2	5				2			54	2	7.0
57	26	12	14	9									61	0	6.0
58	19	17	17	5	6	3				1			68	1	7.3
59	25	9	12	7	6	3		1					63	1	6.8
60	25	19	12	2	5	3							66	0	6.4
61	23	22	14	7	4	3	4						77	0	6.6
62	19	14	11	5	5	2	1			1		1	59	2	7.6
63	19	22	14	3	4								62	0	6.2
64	23	16	15	6	5	1	2						68	0	6.6
65	25	14	14	2	3	1	2						61	0	6.6
66	24	23	11	5	6	1	2	1					73	1	6.8
67	22	30	15	4	1	1	2	1					66	1	6.8
68	25	15	16	8	4	2	1						71	0	6.6
69	23	21	20	8	7	2	1						82	0	6.6
70	19	16	15	5	2	1	1	1					60	1	6.8

STUDY OF SEQUENCES OF EARTHQUAKES IN SYNTHETIC CATALOGS

Block structures considered. The dynamics of three block structures (BS1, BS2, and BS3) shown in Figure 10 was simulated. On the upper plane each of them is a square with a side of 320 km divided by faults into smaller squares. The depth of the layer is $H = 20$ km. The values of parameters for all the faults of the structures are the following: $\alpha = 85^\circ$ (a dip angle); $K = 1$ bar/cm; $V = 0.05$ cm/bars; $V_s = 10$ cm/bars; $B = 0.1$; $H_f = 0.085$; $H_s = 0.07$. The values of parameters for all the faults of the structures are the following: $K_u = 1$ bar/cm; $V_u = 0.05$ cm/bars. The difference between lithostatic and hydrostatic pressure P in formula (11) equals 2 Kbars.

The same movement of boundaries was specified for the all structures. The sides of the largest squares move progressively with the velocity of 10 cm. The directions of the velocities of the boundaries are shown in Figure 1. The angle between the vector of the velocity and the proper side of the square is 10° . The underlying medium does not move.

Numerical modeling of dynamics of the structures were carried out with $\Delta t = 0.001$. The earthquakes were formed from the cells in which failures occurred at the same time and which belonged to a connected set of segments of the same fault. Magnitudes of the earthquakes were calculated with $D = 0.98$ and $E = 3.93$ in (14).

Results of calculations with different space steps. In the first variants different time moments were not attributed to different steps of the given above procedure of recalculation of inelastic displacements after the failure occurrence. Therefore the cells in which failures occurred were united to form earthquake apart from the step of this procedure when it happened.

The calculations were made for two values of the space step: $\epsilon = 5$ km and $\epsilon = 2.5$ km. Table 6 contains the number of earthquakes for different magnitude ranges in the synthetic catalogs obtained with the zero initial conditions for the three structures considered. The data in Table 6 belong to the period between 200 and 400 units of the non-dimensional time. This period was selected to exclude unstable initial part of the simulation. The accumulative frequency-magnitude relations obtained for the synthetic catalogs for the same time period are shown in Figure 11.

TABLE 6 Number of earthquakes in the synthetic catalogs

Magnitude range	Structure and value of ϵ					
	BS1		BS2		BS3	
	5 km	2.5 km	5 km	2.5 km	5 km	2.5 km
$M < 5.0$	0	4744	0	6711	0	7321
$5.0 \leq M < 5.5$	3995	3374	5150	5267	5289	5272
$5.5 \leq M < 6.0$	2881	2721	3930	4708	4242	4896
$6.0 \leq M < 6.5$	1968	1577	2495	2388	2380	2229
$6.5 \leq M < 7.0$	934	916	811	869	661	602
$7.0 \leq M < 7.5$	418	435	295	280	146	156
$M \geq 7.5$	1	2	0	0	0	0
TOTAL	10197	13769	12681	20223	12718	20476

It follows from Table 6 and Figure 11 that:

1) decreasing of the step of space discretization increases the number of earthquakes in the synthetic catalogs; this is mainly connected with appearance of the earthquakes with magnitudes smaller than 5.0 which is due to the smaller size of the cells in the case of $\epsilon = 2.5$ km;

2) if $M \geq 5.0$ then the number of earthquakes and the frequency-magnitude relations in logarithmic scale for all structures do not differ essentially for the different values of ϵ (Fig.11a-11c) values of ϵ ; the slope of the curve seems to increase while the structure complexity increases (Fig.11d);

3) for the both values of ϵ the number of earthquakes with $M < 6.0$ increases while the structure complexity increases and the number of earthquakes with $M \geq 6.5$ decreases at the same time; if $6.5 \leq M < 7.0$ the number of earthquakes is maximum for BS2.

The further analysis was made for the synthetic catalogs obtained with $\epsilon = 2.5$ km.

Sequences of earthquakes. If different time moments are attributed to different steps of the procedure of recalculations after the failure occurrence then time sequences of earthquakes or groups of earthquakes are obtained instead of one earthquake or a group of earthquakes occurring at the same time.

The strongest earthquake in the sequence can be interpreted as a main shock and the other earthquakes as foreshocks and aftershocks. Table 7 contains the total number of earthquakes and the number of main shocks for different magnitude ranges in the synthetic catalogs obtained when different time moments were attributed to different steps of the procedure of recalculation of inelastic displacements.

Note that the number of earthquakes with $M < 5.5$ increases for the both catalogs while the structure complexity increases and the number of earthquakes with $M \geq 6.0$ decreases at the same time. If $5.5 \leq M < 6.0$ the number of earthquakes in the both catalogs is maximum for BS2.

The accumulative frequency-magnitude relations for the synthetic catalogs with the earthquake sequences detected and for the catalogs of main shocks are shown in Figure 12. The curves for the catalogs obtained with $c = 2.5$ km without detecting of the sequences (Fig.11) are also given here for comparison.

Note that the curve in Figure 12a for the catalog obtained for BS1 without detecting of the sequences looks essentially more similar with a straight line than other curves. The curves for the synthetic catalogs with the earthquake sequences detected and for the catalogs of main shocks have the similar shapes.

The histograms of the number of events for the catalogs of main

TABLE 7 Number of earthquakes in the synthetic catalogs when the sequences of earthquakes are detected

Magnitude range	Structure and catalog					
	BS1		BS2		BS3	
	Total	Main shocks	Total	Main shocks	Total	Main shocks
$M < 5.0$	9521	4986	15785	6874	16758	7573
$5.0 \leq M < 5.5$	9207	3820	14914	5739	16097	6162
$5.5 \leq M < 6.0$	8124	2714	12171	4769	10521	4629
$6.0 \leq M < 6.5$	4347	1399	3092	1278	1962	807
$6.5 \leq M < 7.0$	989	390	314	170	281	123
$M \geq 7.0$	26	26	8	8	6	6
TOTAL	32214	13335	46284	18838	45625	19300

shocks for different magnitude intervals and time periods are shown in Tables 8-10. One unit of the non-dimensional time is interpreted as 100 days in these histograms. Magnitude and time steps are 0.2 and 2 years respectively.

These histograms show that the seismic flow does not have a long-term trend but the number of earthquakes for two years changes in 2 times and more. The maximum variations are in the catalog of main shocks for BS1.

Tables 11-13 show for the catalogs of main shocks the histograms for different magnitude intervals of the number of events in accordance with the number of aftershocks which they have. Tables 14-15 show the analogous histograms in accordance with the number of foreshocks.

It follows from these histograms that for the all three structures the number of main shocks without aftershocks is smaller than the number of main shocks without foreshocks. If n is small ($n \leq 3$ for BS1, $n \leq 6$ for BS2, $n \leq 4$ for BS3) then the number of main shocks with n aftershocks is greater than the number of main shocks with n foreshocks. If n is larger then the situation is contrary. If $n > 3$ the main part of the main shocks with n aftershocks or foreshocks belongs to the magnitude ranges $6.0 < M < 6.8$ (BS1), $5.6 < M < 6.2$ (BS2), and $5.4 < M < 6.0$ (BS3). Generally the distributions of the number of aftershocks and foreshocks look similar and do not change essentially from one structure to another.

Conclusions. For the block structures considered the procedure of recalculation of inelastic displacements after the failure occurrence consists generally of several steps. The number of the steps for one procedure can be several tens. If these steps are distinguished then the number of events in the synthetic catalog increases in more than two times. In this case the curve of the frequency-magnitude relation in the logarithmic scale for the simplest structure differs essentially of a strait line. This difference remains for the catalog of main shocks.

TABLE 8 Histogram of the dependence of the number of events on magnitude for the catalog of main shocks obtained for BS1; $\Delta M = 0.2$, $\Delta t = 2$ years

Time	Magnitude																
	4.60	5.00	5.40	5.80	6.20	6.60	7.00	7.40									
1904 - 1905	38	36	25	32	25	7	3	4	8	9	5	4	196
1906 - 1907	71	35	36	64	51	24	28	31	21	20	6	3	390
1908 - 1909	88	47	26	49	41	28	13	21	17	17	5	3	2	.	.	.	357
1910 - 1911	92	50	39	33	38	24	23	20	18	11	8	5	1	.	.	.	360
1912 - 1913	71	44	27	33	24	19	20	16	8	11	14	3	1	.	.	.	291
1914 - 1915	82	47	38	39	58	20	31	41	22	6	6	5	395
1916 - 1917	146	81	53	93	71	42	35	20	18	17	10	1	1	.	.	.	588
1918 - 1919	191	114	52	85	112	64	42	23	16	9	5	4	1	.	.	.	718
1920 - 1921	199	105	78	107	131	67	37	32	14	9	10	3	1	.	.	.	793
1922 - 1923	269	172	108	131	139	51	58	39	18	9	4	2	1	.	.	.	1001
1924 - 1925	230	104	87	84	105	48	47	35	27	18	3	.	1	.	.	.	789
1926 - 1927	87	50	31	40	61	31	27	24	14	13	10	2	1	.	.	.	391
1928 - 1929	76	68	36	49	60	41	41	31	17	10	7	4	440
1930 - 1931	81	45	26	21	26	16	26	20	15	13	5	3	297
1932 - 1933	147	77	48	66	55	38	39	34	22	8	5	4	2	.	.	.	545
1934 - 1935	139	78	47	63	77	35	26	44	19	6	5	2	2	1	.	.	544
1936 - 1937	91	43	32	37	49	33	43	31	19	14	7	1	1	.	.	.	401
1938 - 1939	111	54	37	63	75	34	30	32	23	9	5	4	477
1940 - 1941	100	54	35	59	66	26	23	27	17	14	7	3	1	.	.	.	432
1942 - 1943	106	50	37	42	58	30	32	22	13	6	9	4	2	.	.	.	411
1944 - 1945	48	28	20	27	44	33	15	22	14	15	6	5	1	.	.	.	278
1946 - 1947	83	57	39	66	69	36	45	23	26	17	4	1	466
1948 - 1949	199	96	84	69	132	63	57	39	18	9	7	1	774
1950 - 1951	123	82	60	62	77	49	37	26	13	17	9	4	559
1952 - 1953	106	58	55	36	70	23	18	16	13	8	8	4	2	.	.	.	417
1954 - 1955	107	72	41	56	68	37	28	18	6	5	8	6	3	.	.	.	455
1956 - 1957	44	19	16	20	52	27	23	15	17	11	10	3	1	.	.	.	258
1958 - 1959	59	36	16	39	42	31	40	27	10	6	3	3	312

3184 1802 1229 1565 1876 977 887 733 463 317 189 87 25 1 0																	

13335 events

TABLE 9 Histogram of the dependence of the number of events on magnitude for the catalog of main shocks obtained for BS2; $\Delta M = 0.2$, $\Delta t = 2$ years

Time	Magnitude																
	4.60	5.00	5.40	5.80	6.20	6.60	7.00	7.40									
1904 - 1905	84	31	26	34	48	27	38	22	14	3	4	.	1	.	.	.	332
1906 - 1907	97	70	50	61	68	39	36	30	20	7	1	1	2	.	.	.	482
1908 - 1909	98	59	35	41	96	43	49	38	22	6	2	1	490
1910 - 1911	234	104	62	121	142	58	64	31	11	5	2	2	836
1912 - 1913	177	110	68	82	124	75	61	35	19	1	5	1	758
1914 - 1915	199	119	126	139	212	67	66	35	15	5	.	.	2	.	.	.	985
1916 - 1917	227	135	103	116	162	82	64	20	9	6	2	4	930
1918 - 1919	239	124	100	145	189	82	72	26	10	7	2	996
1920 - 1921	276	154	75	122	170	63	45	31	9	8	4	1	958
1922 - 1923	258	88	66	99	160	65	46	24	13	6	5	830
1924 - 1925	267	151	108	115	164	64	66	31	5	4	3	.	2	.	.	.	980
1926 - 1927	184	95	61	85	115	70	67	36	15	6	.	1	735
1928 - 1929	105	48	26	52	74	44	54	34	15	3	3	3	461
1930 - 1931	75	58	41	63	84	54	50	28	15	4	4	1	477
1932 - 1933	138	73	63	72	113	37	55	28	5	9	4	3	600
1934 - 1935	148	97	78	83	138	70	79	38	8	4	2	2	747
1936 - 1937	64	51	37	50	89	52	46	21	14	7	4	435
1938 - 1939	71	42	32	58	72	38	35	32	17	7	3	2	409
1940 - 1941	84	38	39	44	72	34	37	25	14	10	2	2	401
1942 - 1943	83	54	37	53	63	29	38	31	24	9	3	424
1944 - 1945	112	66	36	69	105	44	58	35	11	9	3	1	549
1946 - 1947	114	61	53	85	126	65	41	23	5	11	6	590
1948 - 1949	269	141	92	129	138	49	67	22	15	11	4	937
1950 - 1951	272	149	87	116	137	76	56	26	11	5	1	2	938
1952 - 1953	222	129	82	125	174	60	55	29	11	6	3	1	897
1954 - 1955	119	86	59	69	118	64	57	22	6	5	3	3	611
1956 - 1957	107	72	58	87	140	80	68	31	11	6	.	1	661
1958 - 1959	82	64	38	51	60	29	21	24	8	7	4	.	1	.	.	.	389

4405 2469 1738 2366 3353 1560 1491 808 352 177 79 32 8 0 0																	

18838 events

TABLE 10 Histogram of the dependence of the number of events on magnitude for the catalog of main shocks obtained for BS3; $\Delta M = 0.2$, $\Delta t = 2$ years

Time	Magnitude																		
	4.60	5.00	5.40	5.80	6.20	6.60	7.00	7.40											
1904 - 1905	162	90	58	76	72	31	8	8	3	4	4	1	517
1906 - 1907	274	131	103	153	152	54	20	22	11	2	3	1	926
1908 - 1909	178	127	65	102	114	56	37	14	2	2	4	1	1	703
1910 - 1911	133	74	44	91	104	41	46	21	9	6	1	1	571
1912 - 1913	145	82	74	107	164	74	33	11	2	2	3	2	699
1914 - 1915	261	148	86	136	174	72	44	15	7	10	4	957
1916 - 1917	203	92	75	99	123	58	37	14	3	6	2	712
1918 - 1919	119	70	60	75	105	45	27	21	9	6	2	1	540
1920 - 1921	130	73	44	81	154	70	55	18	6	6	2	.	2	641
1922 - 1922	209	82	60	83	113	61	59	25	10	4	5	711
1924 - 1925	233	105	56	100	122	56	43	25	11	5	1	757
1926 - 1927	161	79	57	75	105	40	38	23	12	7	3	600
1928 - 1929	73	43	36	56	93	41	31	17	8	3	2	3	406
1930 - 1931	110	68	51	53	85	46	31	11	7	2	2	1	2	469
1932 - 1933	97	63	43	75	144	63	41	10	9	2	1	2	550
1934 - 1935	191	108	76	125	177	56	52	25	12	4	2	1	829
1936 - 1937	158	91	64	91	129	55	37	32	11	2	1	1	672
1938 - 1939	258	101	53	81	133	62	40	24	6	4	3	1	766
1940 - 1941	115	65	42	72	105	65	33	21	11	4	4	.	1	538
1942 - 1943	114	71	45	85	104	53	51	16	10	4	3	1	557
1944 - 1945	143	80	51	66	122	62	58	25	11	1	1	1	621
1946 - 1947	141	100	63	82	137	66	70	15	6	2	3	2	687
1948 - 1949	224	116	55	80	137	50	41	16	11	6	3	1	740
1950 - 1951	275	112	99	150	173	61	40	14	12	2	.	3	941
1952 - 1953	208	100	85	139	112	66	31	19	9	1	.	2	772
1954 - 1955	200	61	67	98	142	51	30	20	11	3	3	1	687
1956 - 1957	328	155	109	153	225	94	32	15	4	3	1	2	1121
1958 - 1959	164	79	65	91	105	49	42	8	3	3	1	610
	5007	2566	1786	2675	3625	1598	1107	505	226	106	64	29	6	0	0				

19300 events

TABLE 11 Histogram of the dependence for different magnitude intervals of the number of events on the number of aftershocks which they have (the catalog of main shocks obtained for BS1)

Number of aftershocks	Magnitude																		
	4.60	5.00	5.40	5.80	6.20	6.60	7.00	7.40											
0	2950	1467	886	977	985	392	208	103	60	47	26	8	2	8111
1	213	295	276	446	630	342	333	274	156	106	57	46	17	1	3192
2	15	36	49	103	159	135	166	140	93	48	17	13	3	977
3	5	3	11	26	57	53	87	96	55	34	21	6	454
4	.	1	5	8	23	23	45	53	31	23	21	7	3	243
5	.	.	1	2	12	12	19	30	24	31	17	2	150
6	1	.	.	3	5	13	11	16	17	8	10	1	85
7	.	.	1	.	2	2	3	9	5	6	5	2	35
8	1	1	4	4	13	4	4	31
9	2	8	4	7	1	4	1	27
10	1	.	1	.	5	2	9
11	1	1	.	1	3	6
12	1	2	3
13	1	.	.	1	.	1	3
14	1	.	1	2	.	.	1	5
15	0
16	1	1
17	1	1	2
18	0
19	0
20	0
21	0
22	0
23	0
24	1	1
	3184	1802	1229	1565	1876	977	887	733	463	317	189	87	25	1	0				

13335 events

TABLE 12 Histogram of the dependence for different magnitude intervals of the number of events on the number of aftershocks which they have (the catalog of main shocks obtained for BS2)

Number of aftershocks	Magnitude																	
	4.60	5.00	5.40	5.80	6.20	6.60	7.00	7.40										
0	3947	1922	1177	1459	1631	397	295	131	45	26	10	2	2					11044
1	400	433	418	635	1003	553	513	307	130	46	21	9	4					4472
2	45	73	99	158	392	281	308	131	45	33	14	3						1582
3	8	24	31	66	168	138	160	77	35	28	9	7						751
4	3	9	6	19	69	93	76	58	33	16	9	5						396
5	1	8	3	15	39	37	47	43	19	10	5		1					228
6			1	7	21	24	40	24	17	5	4	3						146
7	1		1	2	14	28	17	7	6	2	2							92
8				3	5	11	9	8	10	1	1	1						49
9			1		4	7	7	2	6	2	1		1					31
10			1	1	5	3	2	5	2	1	1							21
11					2	1	2	1		2								8
12					1	1	2	1			1							6
13				1	1		1	1	2									6
14							1		1									2
15																		0
16									1									1
17																		0
18							1											1
19																		0
20								1										1
21																		0
22																		0
23																		0
24																		0
25																		0
26																		0
27											1							1
	4405	2469	1738	2366	3353	1560	1491	808	352	177	79	32	8	0	0	0	0	4405

18838 events

TABLE 13 Histogram of the dependence for different magnitude intervals of the number of events on the number of aftershocks which they have (the catalog of main shocks obtained for BS3)

Number of aftershocks	Magnitude																	
	4.60	5.00	5.40	5.80	6.20	6.60	7.00	7.40										
1	4458	2000	1243	1491	1599	373	204	71	24	8	6	2	1					11480
2	482	460	406	821	1115	592	427	172	67	26	10	9	4					4591
3	50	77	104	212	478	297	164	87	38	22	12	5						1546
4	13	19	20	78	218	137	133	64	39	14	8	1						744
5	3	6	8	40	107	91	75	33	17	10	13	2	1					406
6		3	4	16	57	42	41	32	12	7	2	3						219
7		1	1	10	26	28	23	18	10	4	4							125
8	1			1	15	16	12	13	5	5	2	2						72
9				4	4	9	9	5	6	3	3	1						44
10					2	4	6	3	3	1	2							21
11					2	2	6	3	1			2						16
12					2	3	4		1									10
13					2	2	3	1		2		1						11
14					1	1		1	1		1							5
15									1		1							2
16										1								1
17								1										1
18																		1
19										1								1
20											1	1						2
21																		0
22											1	1						2
	5007	2566	1786	2675	3625	1598	1107	505	226	106	64	29	6	0	0	0	0	5007

19300 events

TABLE 14 Histogram of the dependence for different magnitude intervals of the number of events on the number of foreshocks which they have (the catalog of main shocks obtained for BS1)

Number of foreshocks	Magnitude																		
	4.60	5.00	5.40	5.80	6.20	6.60	7.00	7.40											
0	3181	1638	1022	1155	1219	548	479	344	123	44	11	9764
1	3	142	169	298	417	215	164	153	85	44	10	1	1701
2	.	19	28	83	161	109	109	83	50	46	18	2	4	712
3	.	2	7	17	47	59	42	50	49	47	16	11	7	354
4	.	1	2	10	18	28	39	45	56	42	24	15	2	1	283
5	.	.	.	2	8	12	26	15	35	25	24	16	4	167
6	.	.	1	.	4	3	13	17	23	19	26	14	3	123
7	1	5	9	10	19	10	13	2	69
8	1	3	7	11	8	7	5	2	44
9	1	1	2	2	10	9	14	5	1	45
10	1	2	3	4	2	10	1	23
11	2	1	1	4	7	15
12	1	1	3	2	2	9
13	2	1	1	4	8
14	1	.	1	.	2	4
15	1	.	1	2
16	1	2	3	6
17	2	2
18	1	2	3
19	1	1
		3184	1802	1229	1565	1876	977	887	733	463	317	189	87	25	1	0			

13335 events

TABLE 15 Histogram of the dependence for different magnitude intervals of the number of events on the number of foreshocks which they have (the catalog of main shocks obtained for BS2)

Number of foreshocks	Magnitude																		
	4.60	5.00	5.40	5.80	6.20	6.60	7.00	7.40											
0	4352	2155	1336	1664	2262	899	742	284	65	5	1	13765
1	52	268	296	491	646	334	290	135	48	6	3	2569
2	1	38	69	136	251	153	140	109	52	18	6	3	976
3	.	3	25	54	89	69	123	79	45	24	16	5	532
4	.	4	5	15	52	48	66	69	48	23	15	3	2	350
5	.	.	4	1	22	22	49	49	27	27	6	5	2	214
6	.	1	1	1	15	13	30	29	19	24	8	2	1	144
7	.	.	2	3	7	12	13	22	13	14	8	4	1	99
8	3	4	17	13	8	11	5	4	65
9	1	4	7	6	11	7	3	2	1	42
10	.	.	.	1	4	1	3	6	6	4	1	1	1	28
11	1	.	4	3	2	4	1	1	16
12	1	1	2	2	6
13	1	1	4	2	8
14	2	1	1	1	6
15	2	1	1	4
16	1	1	.	1	4
17	2	2
18	1	.	.	1	2
19	0
20	1	.	.	.	1	2
21	1	.	1	2
22	1	1
23	0
24	0
25	0
26	0
27	0
28	0
29	1	1
		4405	2469	1738	2366	3353	1560	1491	808	352	177	79	32	8	0	0			

18838 events

TABLE 16 Histogram of the dependence for different magnitude intervals of the number of events on the number of foreshocks which they have (the catalog of main shocks obtained for BS3)

Number of foreshocks	Magnitude														
	4.60	5.00	5.40	5.80	6.20	6.60	7.00	7.40							
0	4982	2200	1392	1830	2464	820	475	172	33	5	1	1	14375		
1	23	320	300	576	677	274	193	80	29	10	3	.	2485		
2	2	37	68	181	233	188	142	62	38	9	10	1	971		
3	.	9	18	46	121	131	96	54	38	23	7	2	546		
4	.	.	7	26	67	77	73	52	25	17	9	9	364		
5	.	.	.	9	28	44	54	33	25	15	7	5	221		
6	.	.	.	5	23	26	34	22	15	4	8	3	141		
7	.	.	.	2	4	13	11	9	7	5	5	2	59		
8	4	11	9	8	5	6	7	.	50		
9	.	.	1	.	1	7	9	8	5	5	4	2	42		
10	1	3	2	2	1	1	.	2	12		
11	1	1	2	2	.	1	2	.	9		
12	1	2	.	2	5		
13	2	.	1	1	.	1	.	5		
14	2	.	1	3		
15	1	1		
16	2	1	.	2	.	.	.	5		
17	1	.	.	1	.	.	.	2		
18	0		
19	1	1	.	1	.	.	3		
20	1	.	.	.	1		
	5007	2566	1786	2675	3625	1598	1107	505	226	106	64	29	6	0	0

19300 events

REFERENCES

1. Arinei, St. (1974). The Romanian Territory and Plate Tectonics, Technical Publishing House, Bucharest (in Romanian).
2. Mocanu, V.I. (1993). Final report "Go West" Programme. Proposal No: 4609. Contract No: CIPA3S10PL924609. Subject: "Methods for Investigation of Different Kinds of Lithospheric Plates in Europe". Period September-December 1993 (Scientific Supervisor: Prof.G.F.Panza).
3. Radu C.(1979) Catalogue of strong earthquakes originated on the Romanian territory, Part II: 1901-1979, in Seismological Research on the Earthquake of March 4, 1977 - Monograph (eds. I.Cornea and C.Radu, Central Institute of Physics, Bucharest)
4. Earthquakes in the USSR. 1962-1990. M.: Nauka. 1965-1992.
5. Trifu C.-I. and Radulian M. (1991) A depth-magnitude catalog of Vrancea intermediate depth microearthquakes. Rev. Rom. GEOPHYSIQUE. Bukarest, 35. RR 31-45, 1991.

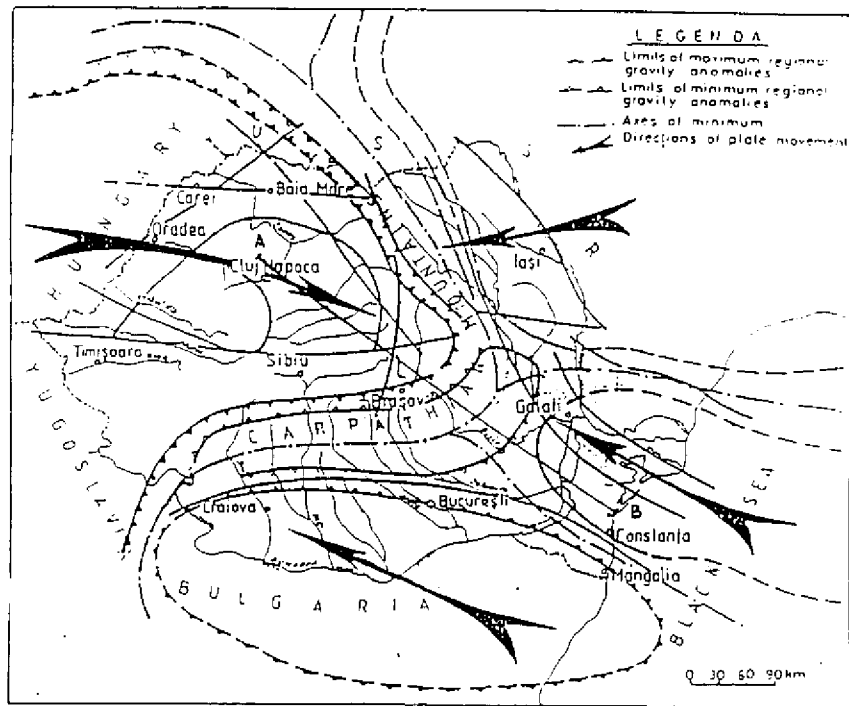


FIGURE 1 Tectonic plates and main geodynamics elements of Romania (taken from [2]).

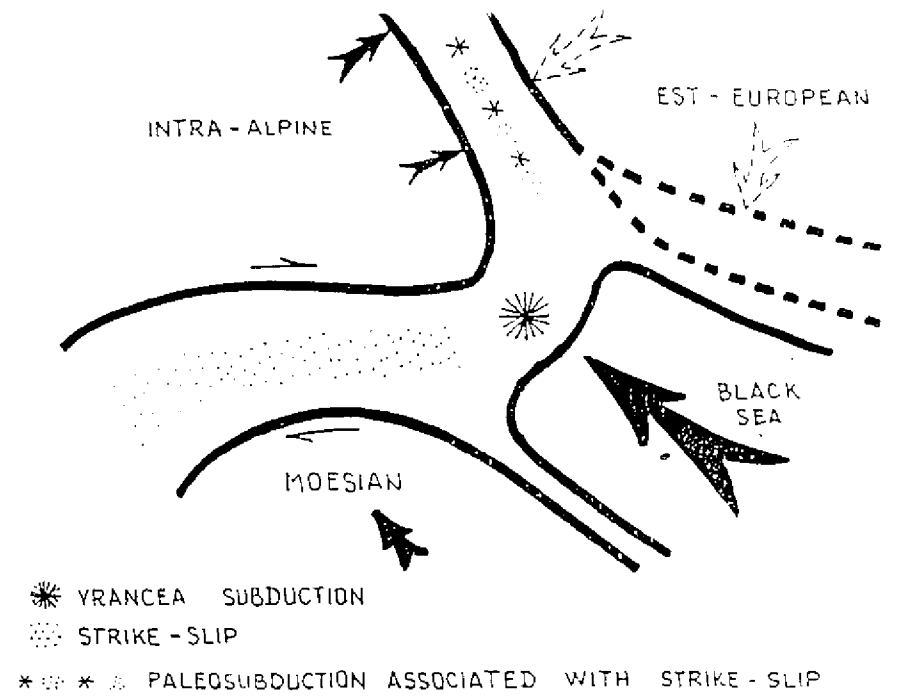


FIGURE 2 The kinematic model proposed for the double subduction process in the Vrancea region (taken from [2]).

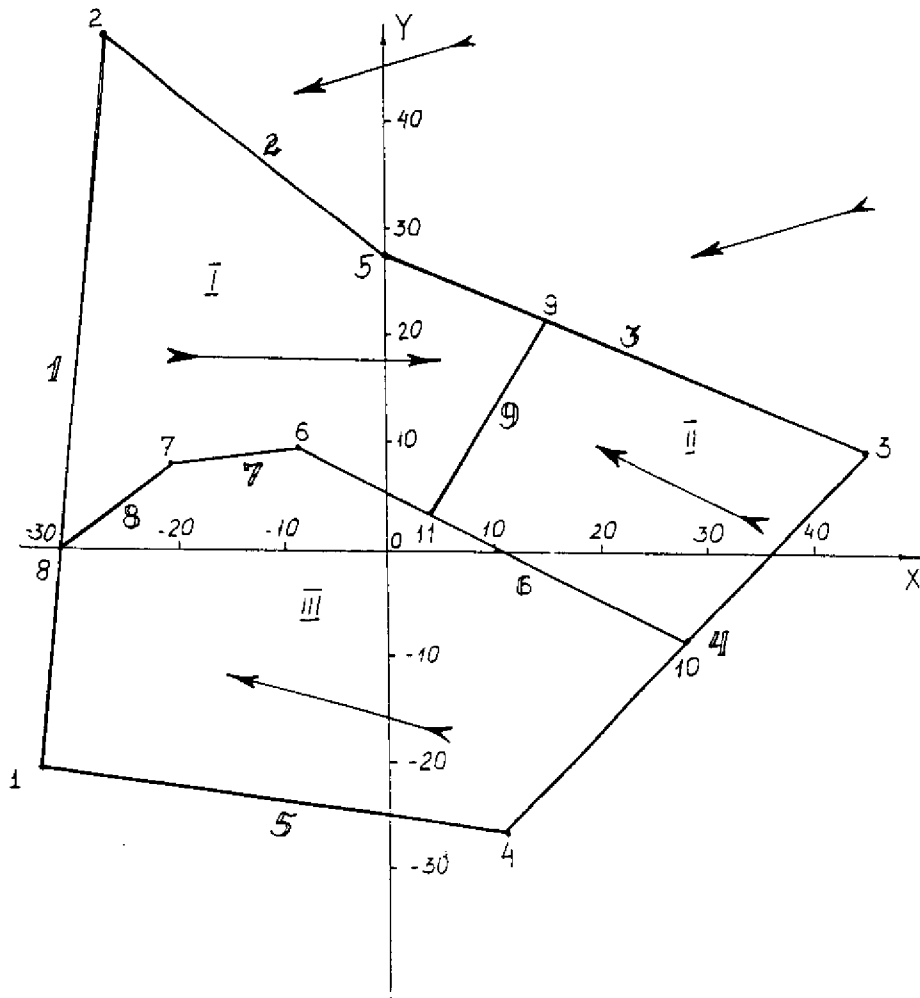


FIGURE 3 The block structure for the numerical simulation; the numbers of the vertices, faults and blocks are indicated.

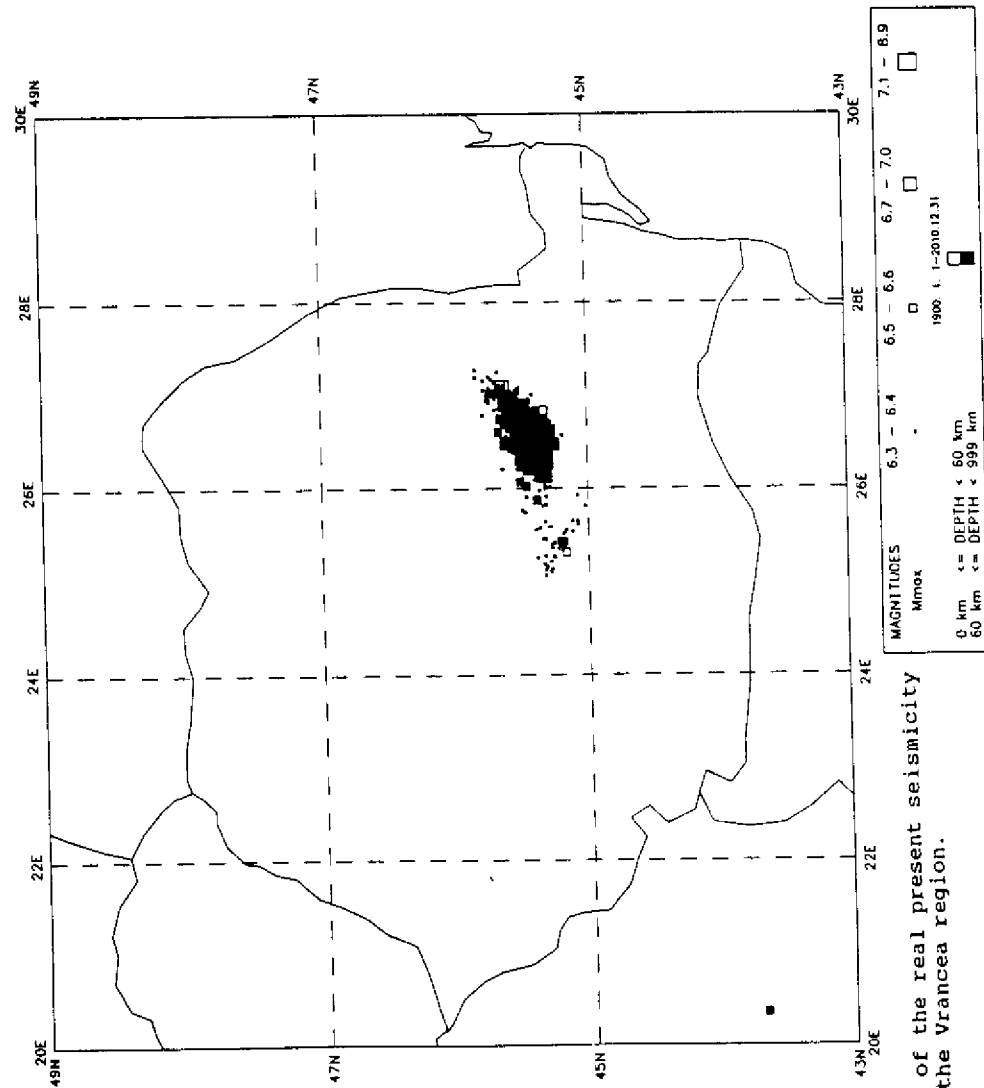


FIGURE 4 Map of the real present seismicity of the Vrancea region.

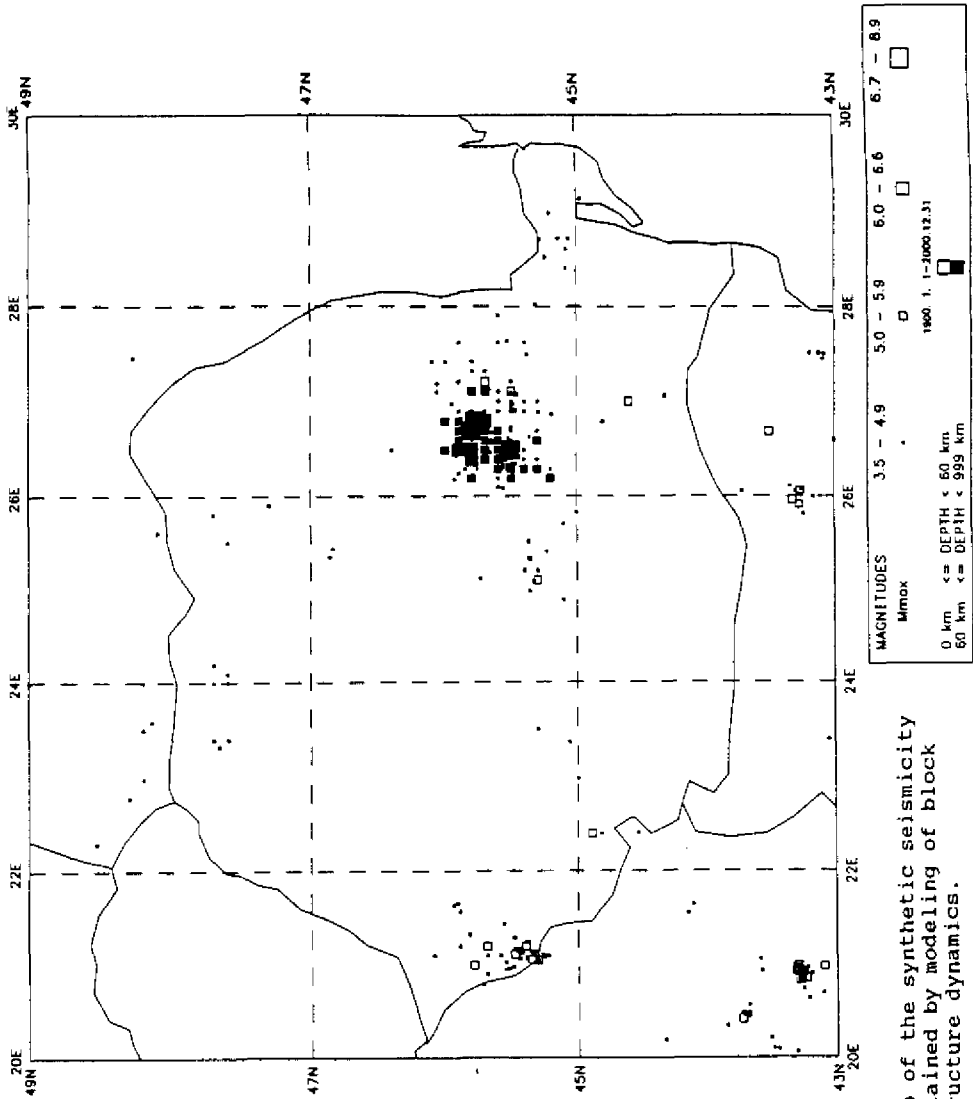


FIGURE 5 Map of the synthetic seismicity obtained by modeling of block structure dynamics.

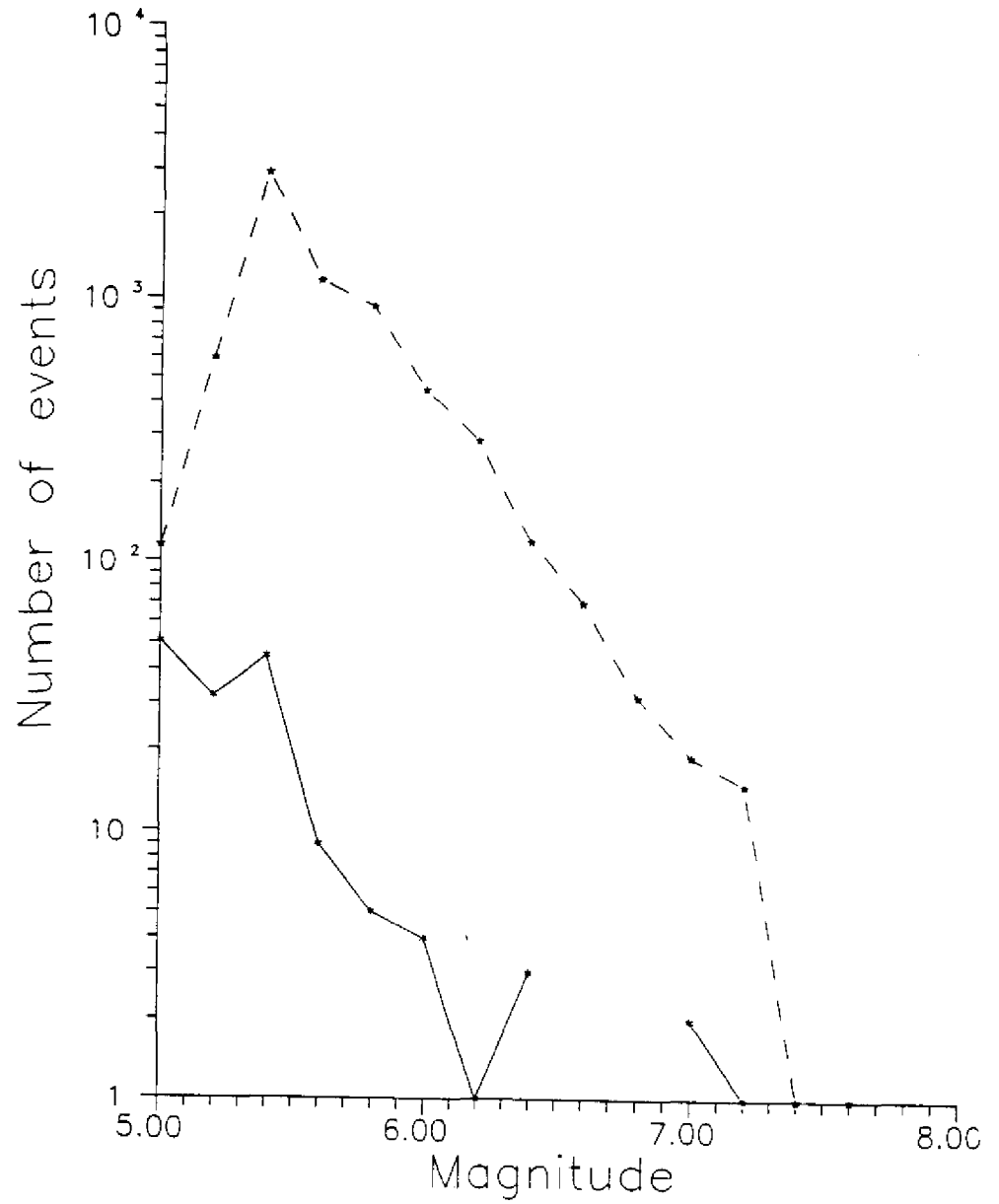


FIGURE 6 Frequency-of-magnitude graphs for the real (the solid line) and synthetic (the dashed line) catalogs.

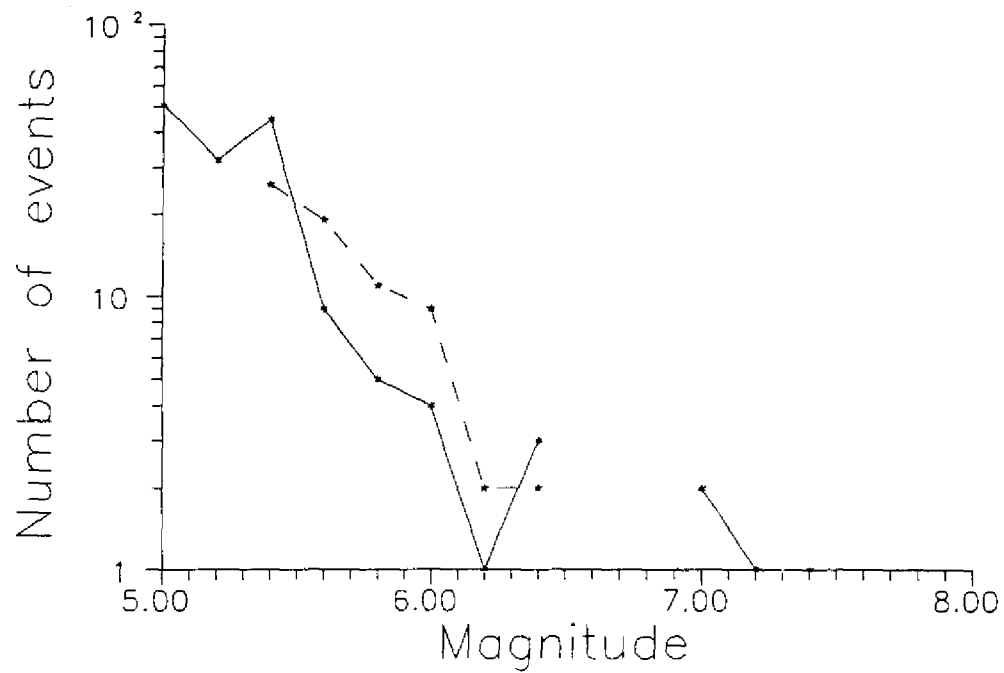


FIGURE 7 Frequency-of-magnitude graphs for the real catalog (the solid line) and for the part of the synthetic catalog for the period without strong earthquakes (the dashed line).

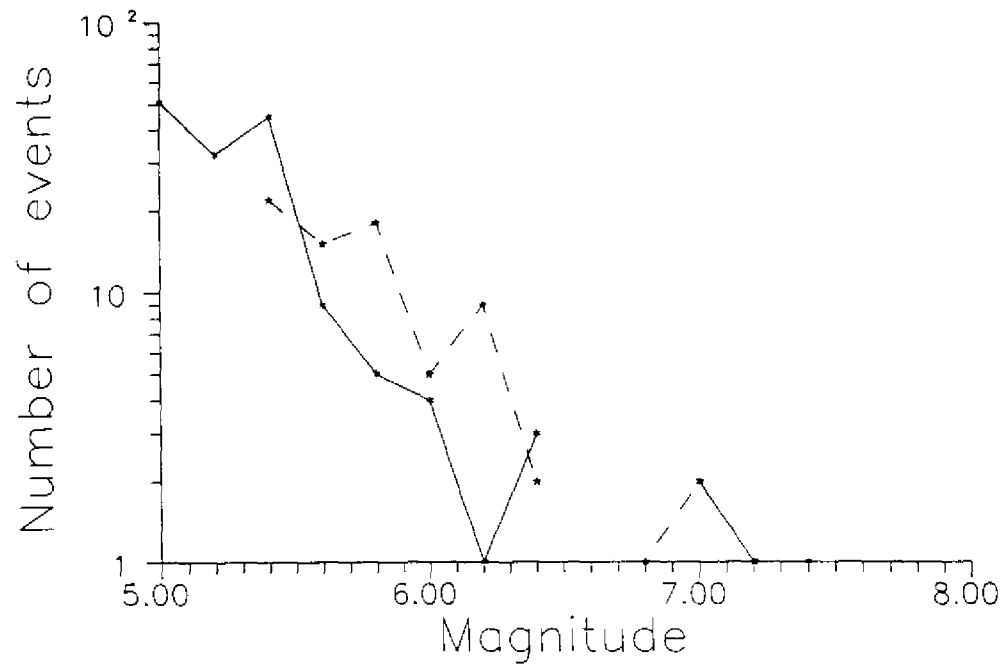


FIGURE 8 Frequency-of-magnitude graphs for the real catalog (the solid line) and for the part of the synthetic catalog for the period with several strong earthquakes (the dashed line).

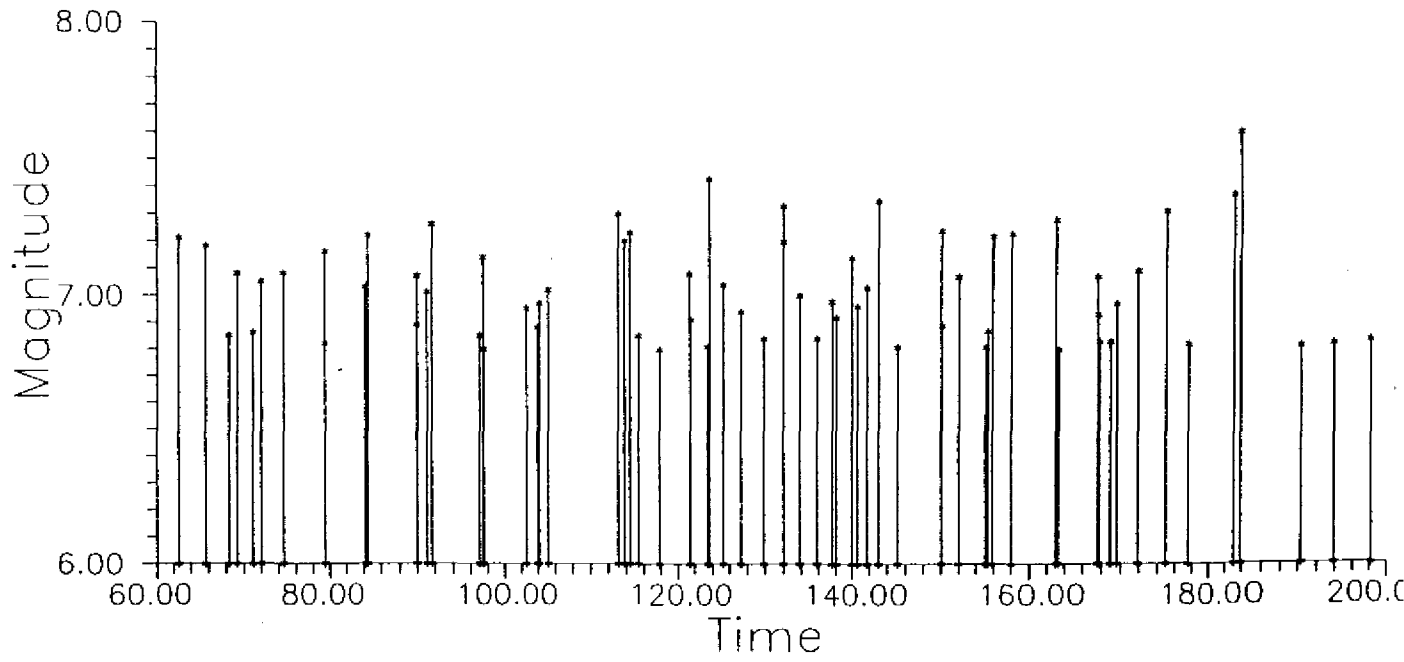


FIGURE 9 Temporal distribution of strong earthquakes in the synthetic catalog for the whole period of time.

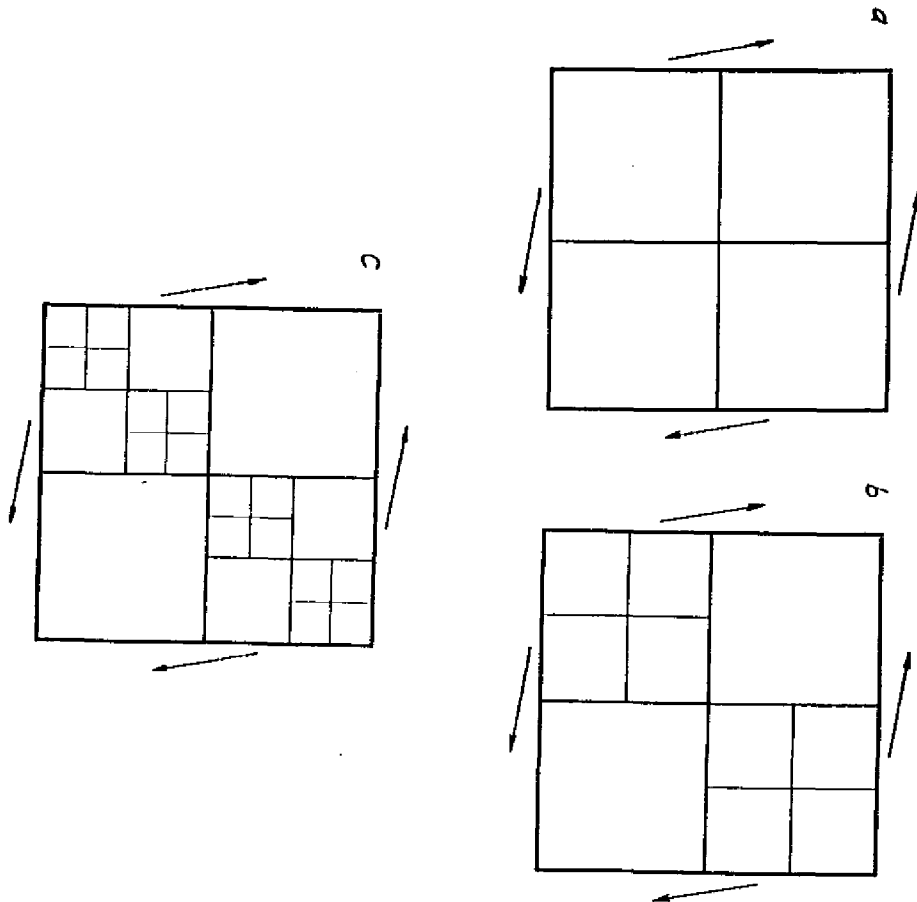


FIGURE 10 The block structures considered:
 a - BS1, b - BS2, c - BS3.

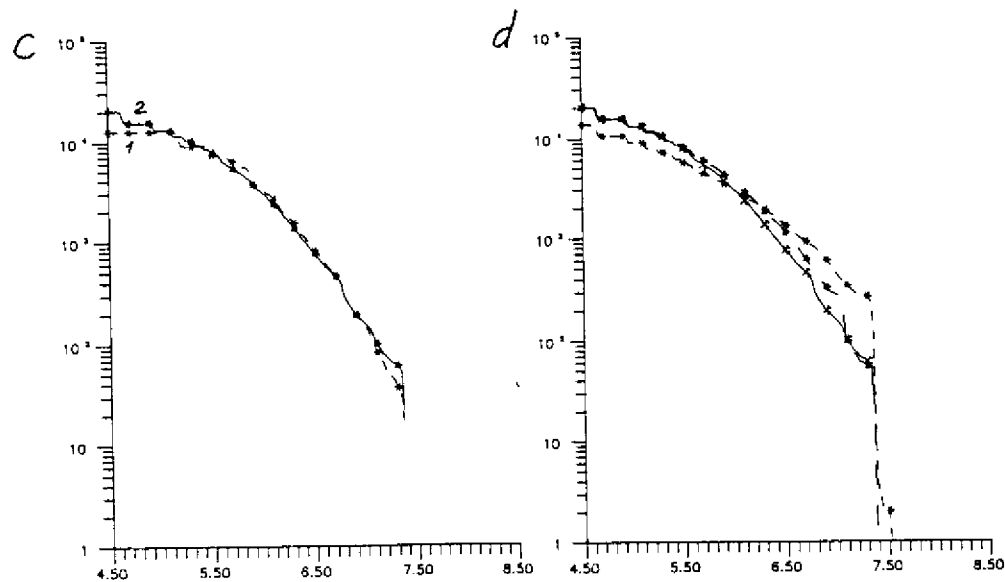
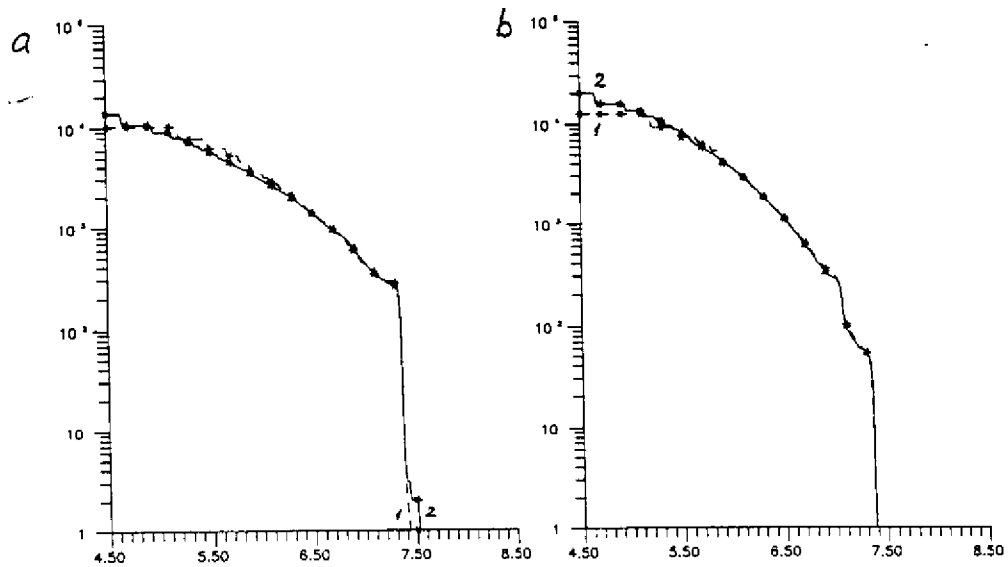


FIGURE 11 The accumulative frequency-magnitude relations for the synthetic catalogs without detection of the earthquake sequences obtained with $\epsilon = 5$ km (1) and $\epsilon = 2.5$ km (2) for BS1 (a), BS2 (b), BS3 (c), and the curves for the three structures for $\epsilon = 2.5$ km (d).

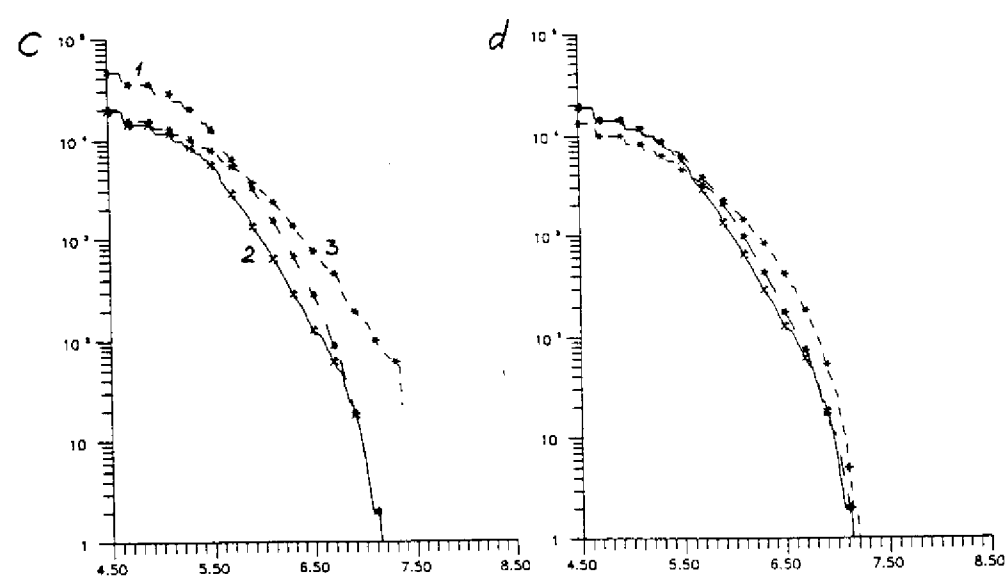
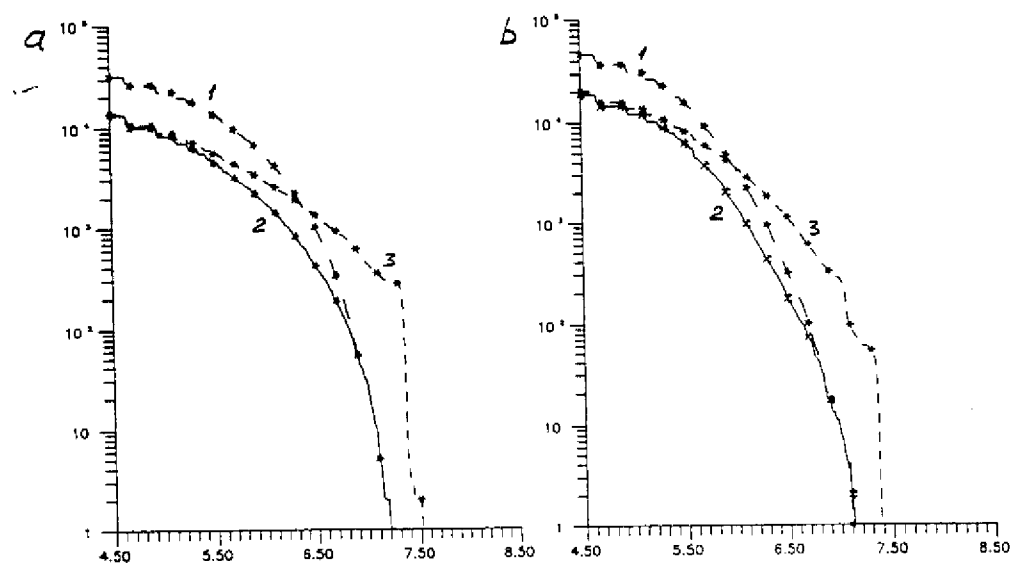


FIGURE 12 The accumulative frequency-magnitude relations for the synthetic catalogs with detection of the earthquake sequences (1), the catalogs of main shocks (2), and the catalogs without detection of the earthquake sequences (3) obtained with $\epsilon = 2.5$ km for BS1 (a), BS2 (b), and BS3 (c) and the curves for the catalogs of main shocks for the three structures (d).